

Supplementary Information

Synthesis of Cryptomelane Type α -MnO₂ (K_xMn₈O₁₆) Cathode Materials with Tunable K⁺ content: The Role of Tunnel Cation Concentration on Electrochemistry

Altug S. Poyraz^a, Jianping Huang^b, Christopher Pelliccione^a, Xiao Tong,^a Shaobo Cheng,^{a,c} Lijun Wu,^a Yimei Zhu,^a Amy C. Marschilok^{b,d*}, Kenneth J. Takeuchi^{b,d*}, and Esther S. Takeuchi^{a,b,d*}

^a Energy Sciences Directorate, Brookhaven National Laboratory, Upton, NY 11973, USA.

^b Department of Chemistry, Stony Brook University, Stony Brook, NY 11794, USA.

^c Department of Materials Science and Engineering, Tsinghua University, Beijing, 100084, China.

^d Department of Materials Science and Engineering, Stony Brook University, Stony Brook, NY 11794, USA.

* Corresponding Authors: (ACM) amy.marschilok@stonybrook.edu, (KJT) kenneth.takeuchi.1@stonybrook.edu, (EST) esther.takeuchi@stonybrook.edu

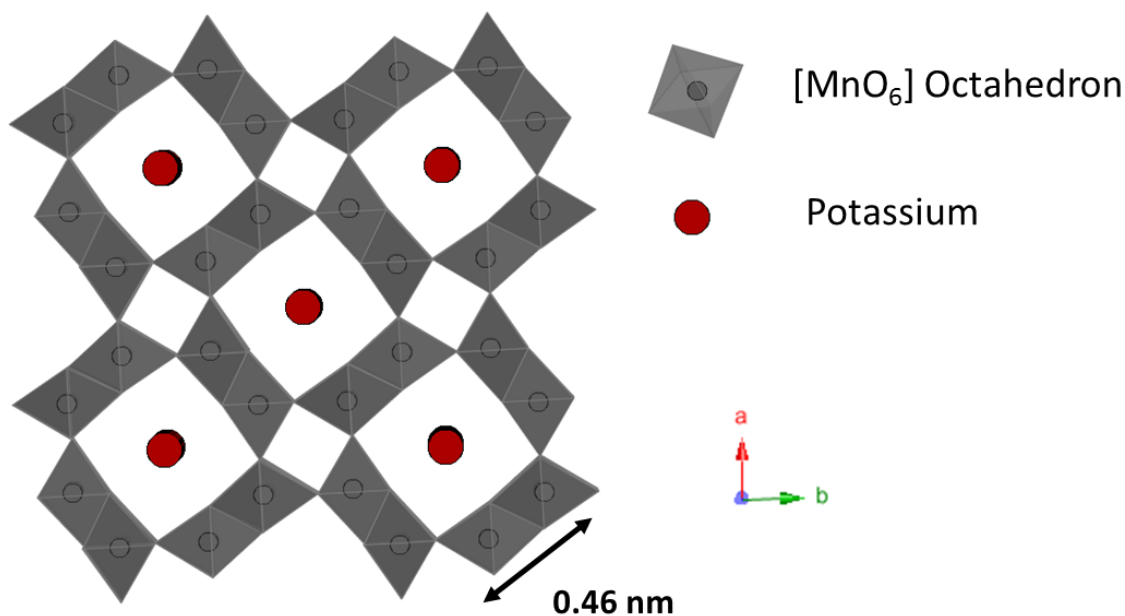


Fig. S1 Schematic structural representation of 2 x 2 (0.46 x 0.46 nm) cryptomelane type manganese dioxide (K_xMn₈O₁₆, α -MnO₂) with space group of I4/m. The structure is along the c axis. Red spheres represent potassium and gray polyhedra represent MnO₆ octahedral units.

Table S1 Lattice Parameters of Potassium ion free and Potassium ion containing Mn_8O_{16} (α - MnO_2 structured) materials from literature

Reference	Composition	a (Å)	c (Å)	Volume (Å ³)
Yang et al. ¹	$\text{Mn}_8\text{O}_{16} \cdot 1.36\text{H}_2\text{O}$	9.7914	2.8633	274.51
	$\text{Mn}_8\text{O}_{16} \cdot 0.88\text{H}_2\text{O}$	9.7732	2.8639	273.56
Kijima et al. ²	$\text{Mn}_8\text{O}_{16} \cdot \text{XH}_2\text{O}$	9.805(4)	2.8510(13)	274.65
Johnson et al. ³	$\text{Mn}_8\text{O}_{16} \cdot 2 \cdot 64\text{H}_2\text{O}$	9.814(3)	2.850(1)	274.5
Johnson et al. ³	$\text{Mn}_8\text{O}_{16} \cdot 2 \cdot 0\text{H}_2\text{O}$	9.8107(8)	2.8502(5)	274.33
	Dehydrated Mn_8O_{16}	9.7502(9)	2.8607(6)	271.96
Gao et al. ⁴	$\text{K}_{0.88}\text{Mn}_8\text{O}_{16} \cdot 0.4\text{H}_2\text{O}$	9.8241(5)	2.8523(1)	275.28
Kadoma et al. ⁵	$\text{K}_{1.12}\text{Mn}_8\text{O}_{16} \cdot 1.2\text{H}_2\text{O}$	9.77(5)	2.85(6)	272.(9)
	$\text{K}_{1.12}\text{Mn}_8\text{O}_{16} \cdot 0.32\text{H}_2\text{O}$	9.78(0)	2.85(4)	273.(0)
	$\text{K}_{1.12}\text{Mn}_8\text{O}_{16} \cdot 0.0\text{H}_2\text{O}$	9.75(6)	2.85(6)	271.(8)

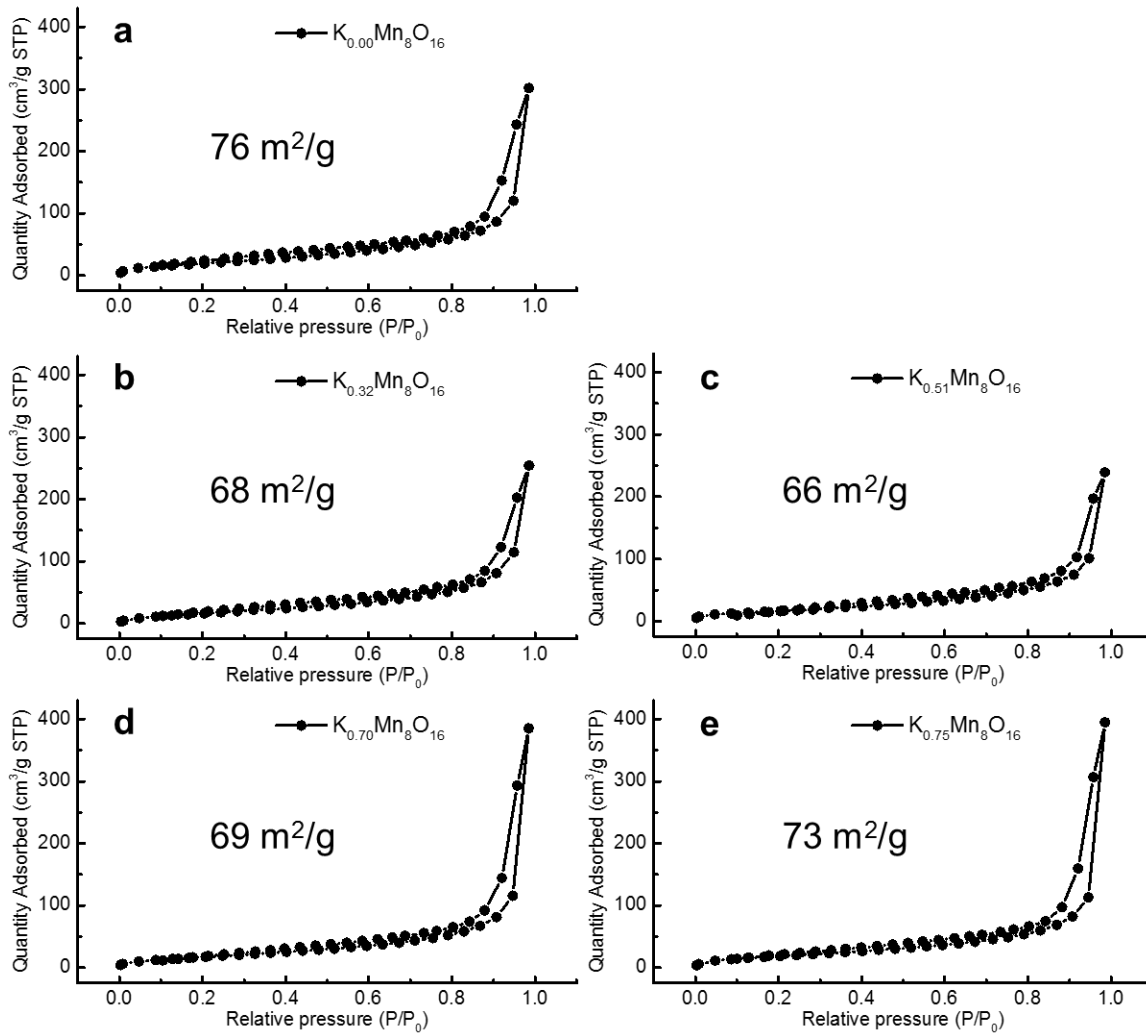


Fig. S2 Nitrogen adsorption-desorption isotherms of $K_xMn_8O_{16}$ samples, where $x = 0.00, 0.32, 0.51, 0.70,$ and 0.75 .

Table S2 Parameters from Rietveld refinement for $K_{0.00}Mn_8O_{16}$, $K_{0.32}Mn_8O_{16}$, and $K_{0.75}Mn_8O_{16}$ samples. Wyckoff positions and Mn-O distances and angles. Debye-Waller factors are shown as Biso values

$K_{0.00}Mn_8O_{16}$	Atom	Wyckoff	X	Y	Z	Biso
	Mn	8h	0.3546(3)	0.1704(2)	0	0.0046(7)
	O1	8h	0.1391(9)	0.1959(6)	0	0.006(3)
	O2	8h	0.185(1)	0.475(1)	0	0.018(3)
$K_{0.32}Mn_8O_{16}$	Atom	Wyckoff	x	y	z	Biso
	K	4e	0	0	0.40(2)	0.03(3)
	Mn	8h	0.3520(3)	0.1686(3)	0	0.0079(6)
	O1	8h	0.1420(9)	0.2018(6)	0	0.013(3)
	O2	8h	0.531(1)	0.1834(8)	0	0.014(3)
$K_{0.75}Mn_8O_{16}$	Atom	Wyckoff	x	y	z	Biso
	K	4e	0	0	0.44(1)	0.027(9)
	Mn	8h	0.3509(2)	0.1675(2)	0	0.0083(5)
	O1	8h	0.1497(8)	0.2035(5)	0	0.016(2)
	O2	8h	0.5370(9)	0.1766(7)	0	0.014(2)

	Mn-O Bond Distances (Å)		
	K_{0.00}Mn₈O₁₆	K_{0.32}Mn₈O₁₆	K_{0.75}Mn₈O₁₆
O1	2.127	2.089	2.008
O2	1.941	1.916	1.909
O3	1.941	1.916	1.909
O4	2.056	2.001	1.938
O5	2.056	2.001	1.938
O6	1.675	1.761	1.83
Average Mn-O	1.966	1.947	1.922
Minimum Angle	84.965	85.083	83.12
Maximum Angle	104.112	103.254	99.868

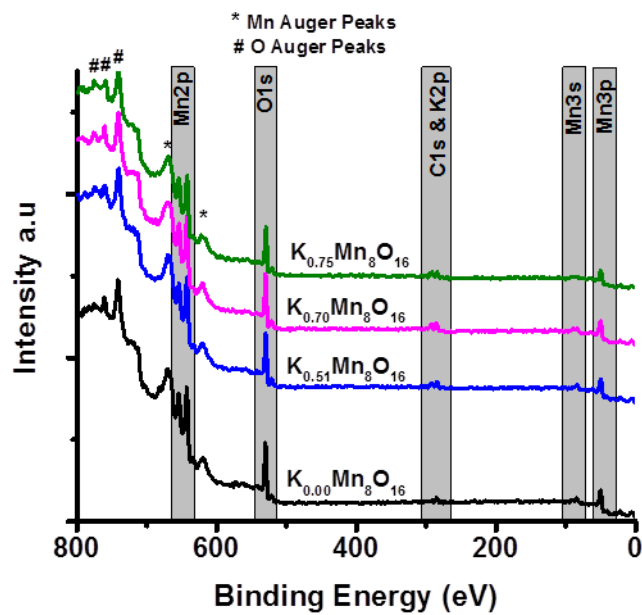


Fig. S3 X-ray Photoelectron (XPS) survey spectra of $K_xMn_8O_{16}$ samples, where $X = 0.00, 0.51, 0.70,$ and 0.75 .

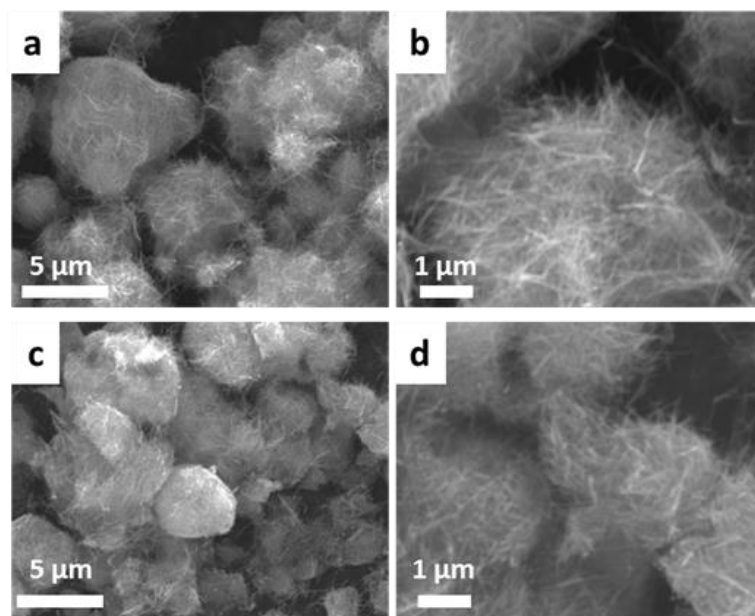


Fig. S4 SEM Images of (a), (b) $K_{0.51}Mn_8O_{16}$ (c), (d) $K_{0.70}Mn_8O_{16}$. The images were recorded at two different magnifications: (a), (c), (e) were at 5kX and (b), (d), (f) were at 15kX.

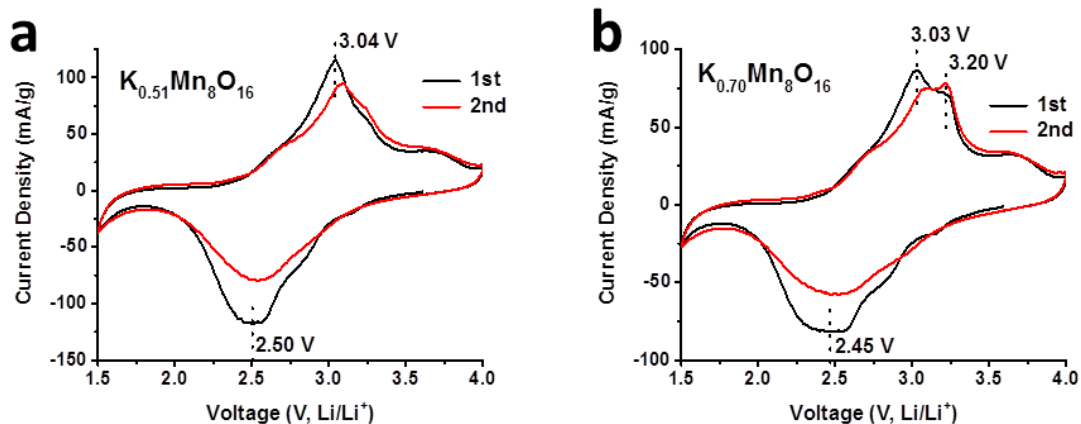


Fig. S5 Cyclic Voltammetry of (a) $K_{0.51}Mn_8O_{16}$ and (b) $K_{0.70}Mn_8O_{16}$. Scan rate is 0.1 mV/s.

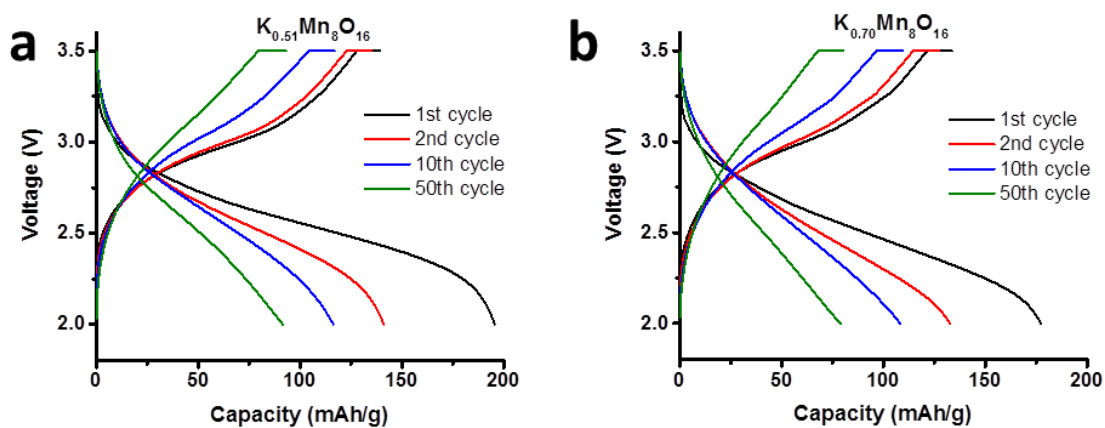


Fig. S6 Representative discharge profiles at cycles 1, 2, 10, and 50 were shown at (a) for $K_{0.51}Mn_8O_{16}$ and (b) for $K_{0.70}Mn_8O_{16}$. The cells were discharged-charged at a rate of 50mA/g.

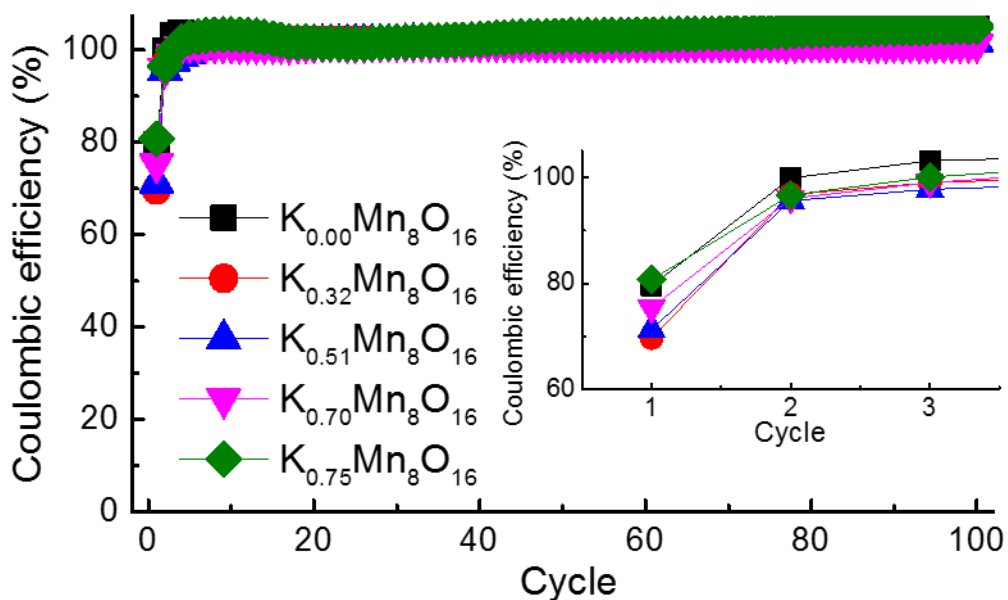


Fig. S7 Coulombic efficiency of $K_xMn_8O_{16}$ samples with varying K^+ content where X = 0.00, 0.32, 0.51, 0.70, and 0.75.

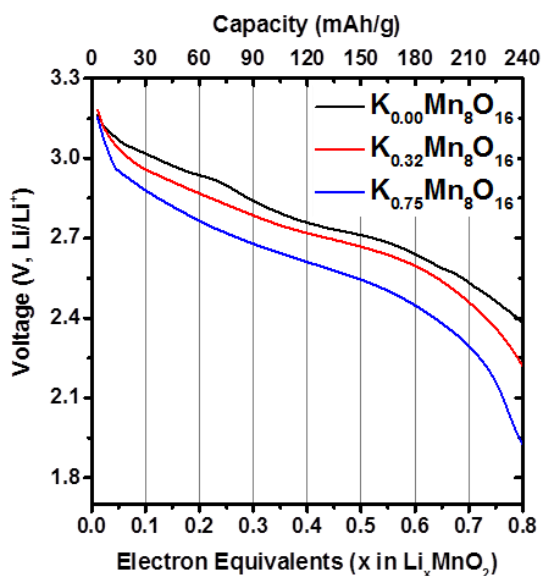


Fig. S8 Open circuit voltage (OCV) plots of $K_{0.00}Mn_8O_{16}$, $K_{0.32}Mn_8O_{16}$, and $K_{0.75}Mn_8O_{16}$. OCVs were recorded at the end of rest period of GITT plots. 100mA/g pulse current for 2 min followed by 5h rest between the pulses.

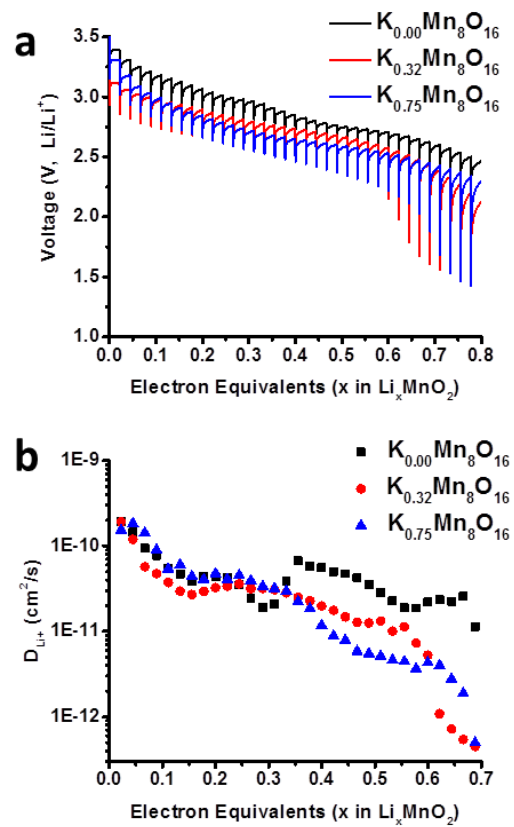


Fig. S9 (a) Galvanostatic Intermittent Titration Technique (GITT) plots and (b) Diffusion coefficient plots of $K_{0.00}Mn_8O_{16}$, $K_{0.32}Mn_8O_{16}$, and $K_{0.75}Mn_8O_{16}$. 40mA/g pulse current for 10 min followed by 12h rest between the pulses.

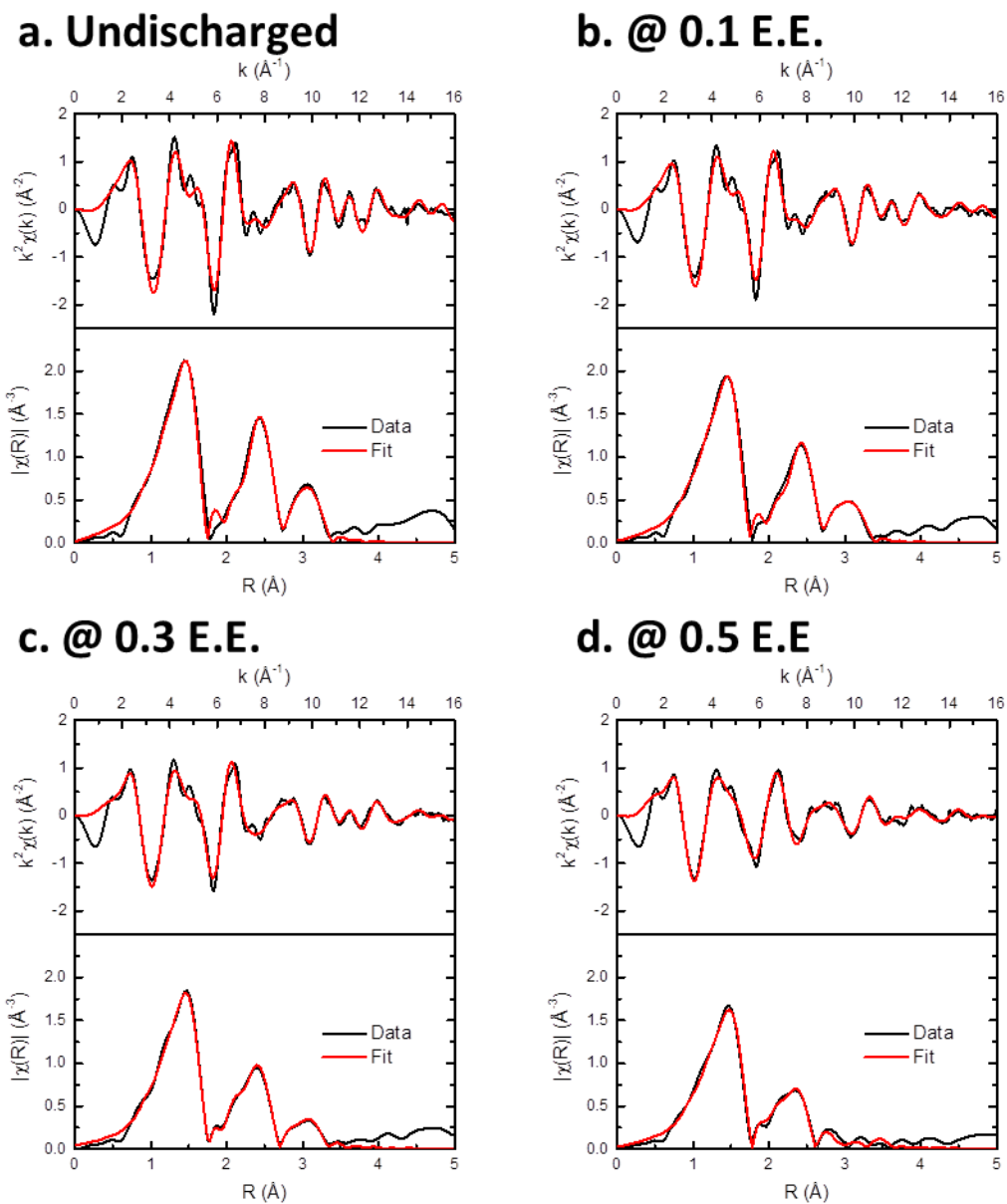
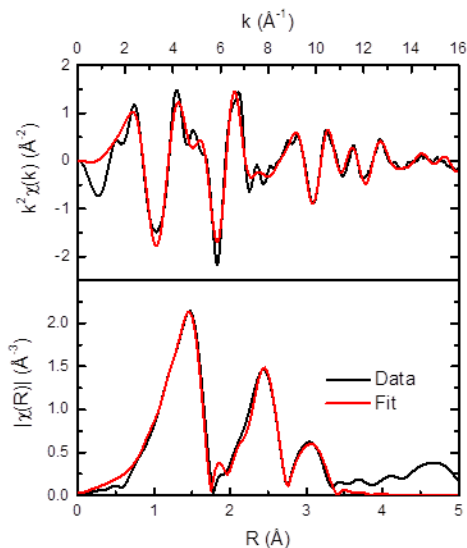
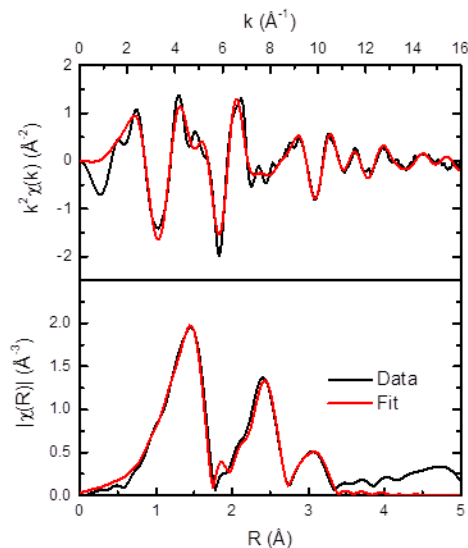


Fig. S10 EXAFS k-space and fitted r-space spectra for $\text{K}_{0.00}\text{Mn}_8\text{O}_{16}$ at 0 (undischarged), 0.1, 0.3, and 0.5 lithiation levels (Electron equivalents per MnO_2). Electron equivalent numbers are reported in per MnO_2 unit.

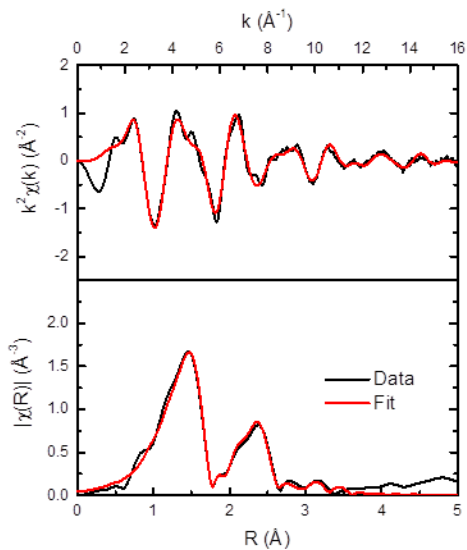
a. Undischarged



b. @ 0.1 E.E



c. @ 0.3 E.E



d. @ 0.5 E.E

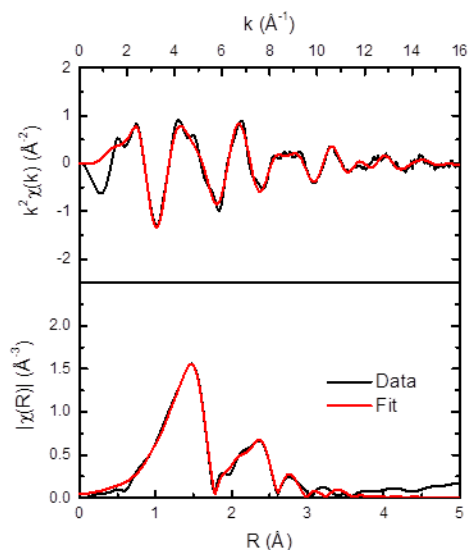


Fig. S11 EXAFS k -space and fitted r -space spectra for $\text{K}_{0.32}\text{Mn}_8\text{O}_{16}$ at 0 (undischarged), 0.1, 0.3, and 0.5 lithiation levels (Electron equivalents per MnO_2). Electron equivalent numbers are reported in per MnO_2 unit.

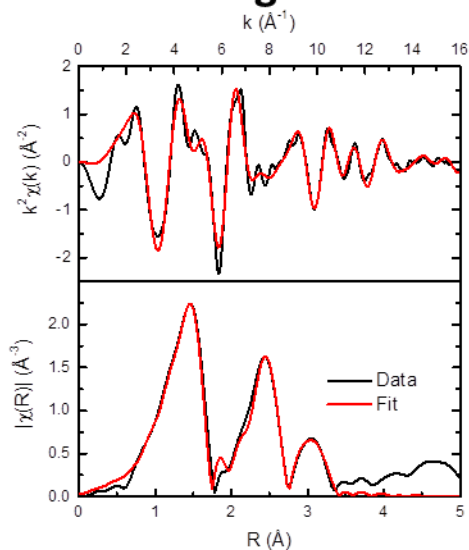
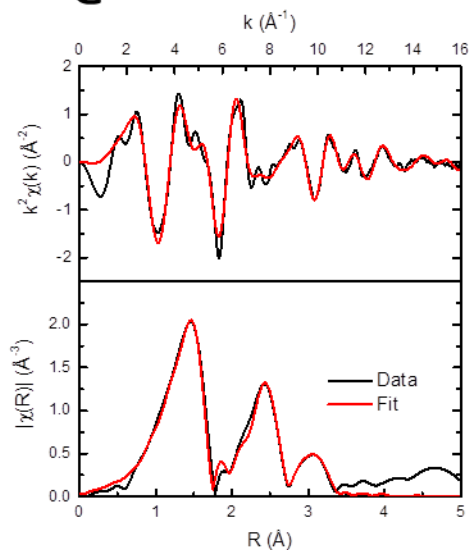
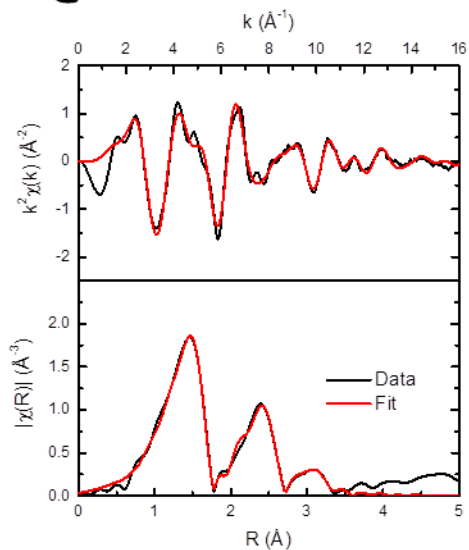
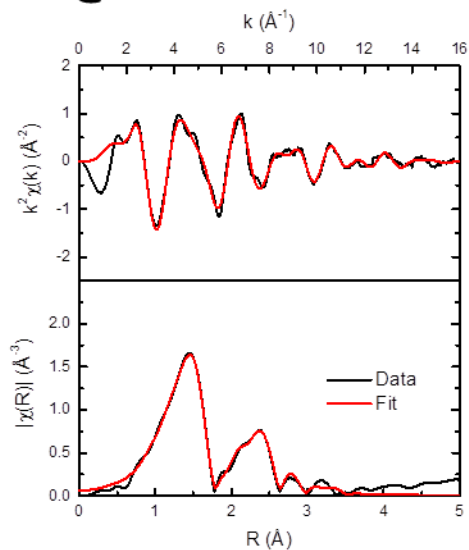
a. Undischarged**b. @ 0.1 E.E.****c. @ 0.3 E.E.****d. @ 0.5 E.E.**

Fig. S12 EXAFS k -space and fitted r -space spectra for $\text{K}_{0.75}\text{Mn}_8\text{O}_{16}$ at 0 (undischarged), 0.1, 0.3, and 0.5 lithiation levels (Electron equivalents per MnO_2). Electron equivalent numbers are reported in per MnO_2 unit.

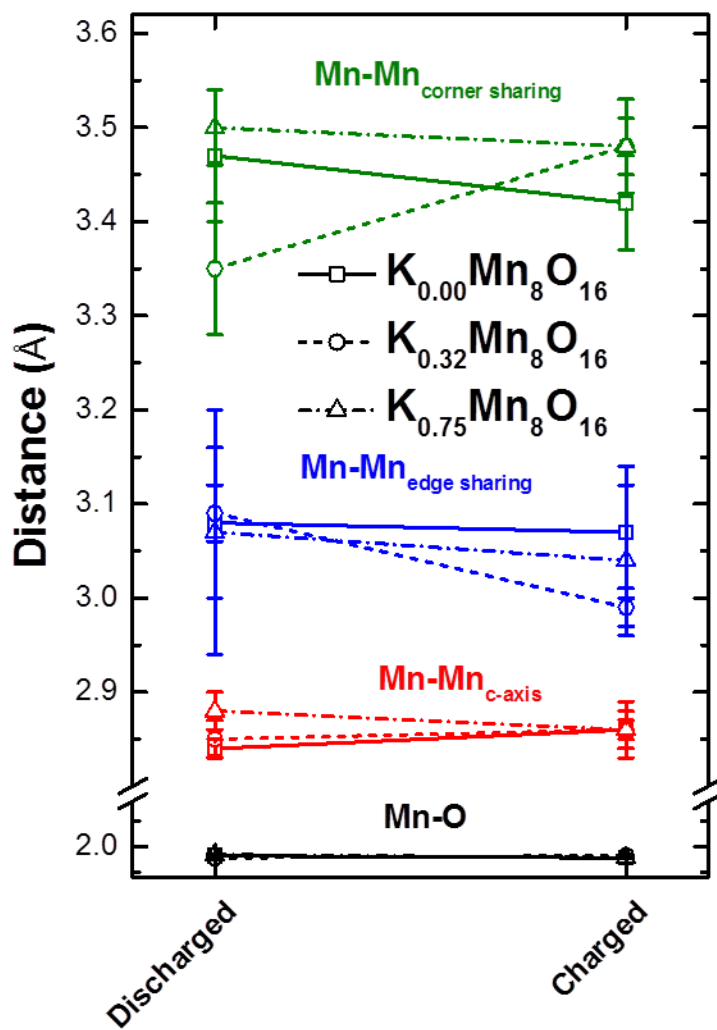


Fig. S13 EXAFS interatomic distance modeling results for $K_{0.00}Mn_8O_{16}$, $K_{0.32}Mn_8O_{16}$, and $K_{0.75}Mn_8O_{16}$ after 50 cycles and at discharged and charged states. Mn-O (black lines) Mn-Mn_{c-axis} (red), Mn-Mn_{edge sharing} and Mn-Mn_{corner sharing} are displayed.

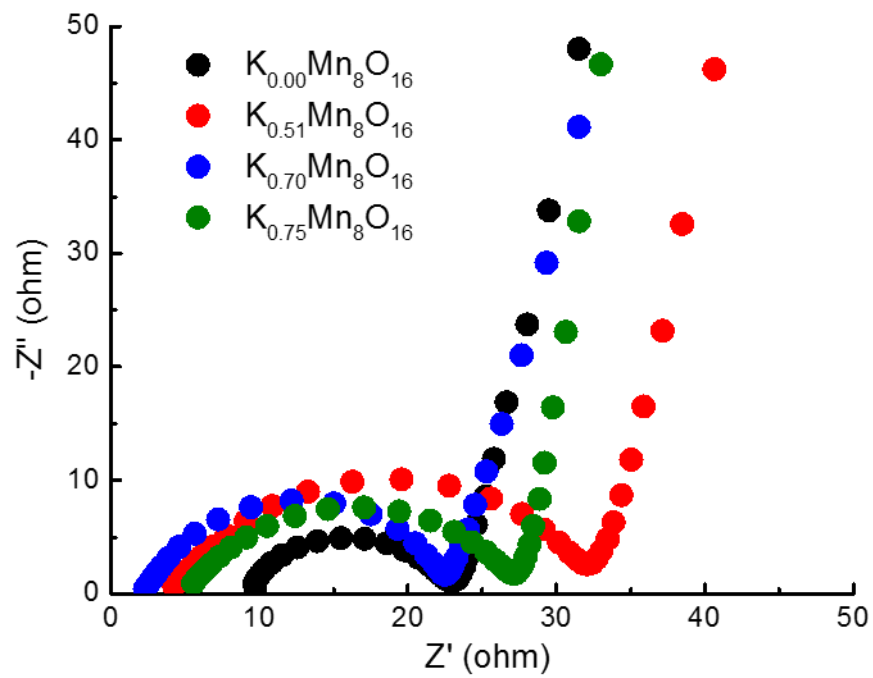


Fig. S14 AC impedance data of $K_xMn_8O_{16}$ samples before discharge.

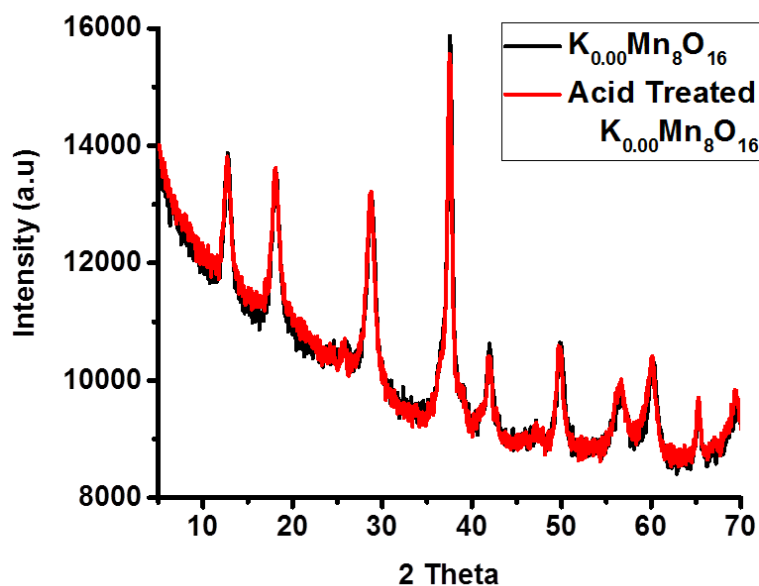


Fig. S15 Powder X-ray diffraction (PXRD) patterns of cation free $K_{0.00}Mn_8O_{16}$ and Acid Treated $K_{0.00}Mn_8O_{16}$. Acid treatment was produced by refluxing $K_{0.00}Mn_8O_{16}$ in 1M HNO_3 at $60^\circ C$ for 72h followed by a heat treatment at $280^\circ C$.

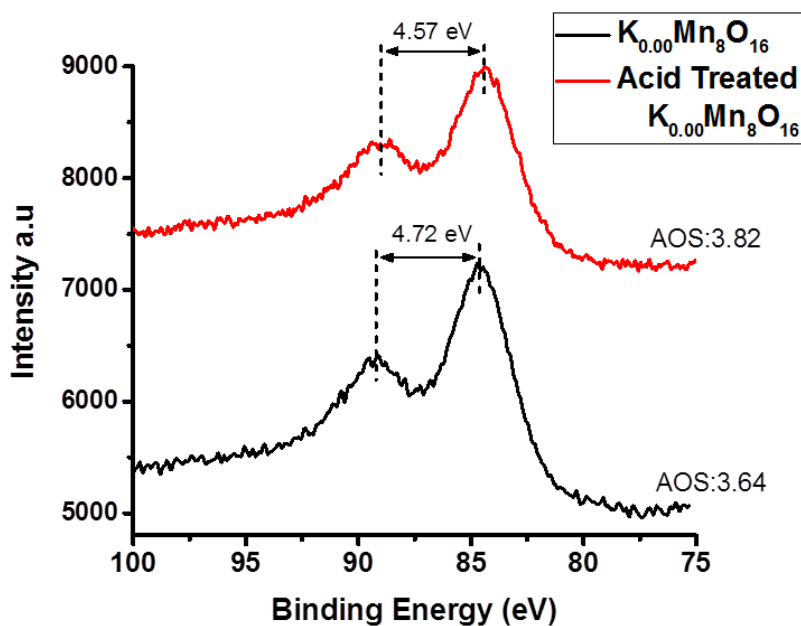


Fig. S16 Mn3s X-ray Photoelectron spectra (XPS) of $K_{0.00}Mn_8O_{16}$ and Acid Treated $K_{0.00}Mn_8O_{16}$ and calculated average oxidation states (AOS) of manganese in these samples, $AOS = 8.956 - 1.126 \times \Delta E(3s)$.

References

1. Z. Yang, L. Trahey, Y. Ren, M. K. Chan, C. Lin, J. Okasinski and M. M. Thackeray, *Journal of Materials Chemistry A*, 2015, **3**, 7389-7398.
2. N. Kijima, H. Yasuda, T. Sato and Y. Yoshimura, *Journal of Solid State Chemistry*, 2001, **159**, 94-102.
3. C. Johnson and M. Thackeray, *Journal of Power Sources*, 2001, **97**, 437-442.
4. T. Gao, M. Glerup, F. Krumeich, R. Nesper, H. Fjellvåg and P. Norby, *The Journal of Physical Chemistry C*, 2008, **112**, 13134-13140.
5. Y. Kadoma, S. Oshitari, K. Ui and N. Kumagai, *Electrochimica Acta*, 2007, **53**, 1697-1702.